Probing Conformational Disorder in Neurotensin by Two-Dimensional Solid-State NMR and Comparison to Molecular Dynamics Simulations

Henrike Heise,* Sorin Luca,* Bert L. de Groot,[†] Helmut Grubmüller,[†] and Marc Baldus*

*Department of NMR-Based Structural Biology and [†]Department of Theoretical and Computational Biophysics, Max-Planck-Institute for Biophysical Chemistry, 37077 Göttingen, Germany

ABSTRACT   An approach is introduced to characterize conformational ensembles of intrinsically unstructured peptides on the atomic level using two-dimensional solid-state NMR data and their combination with molecular dynamics simulations. For neurotensin, a peptide that binds with high affinity to a G-protein coupled receptor, this method permits the investigation of the changes in conformational preferences of a neurotransmitter transferred from a frozen aqueous solution via a lipid model phase to the receptor-bound form. The results speak against a conformational preorganization of the ligand in detergents in which the receptor has been shown to be functional. Further extensions to the study of protein folding are possible.

INTRODUCTION

The structural characterization of unstructured or partially folded peptides and proteins in terms of conformational ensembles is important for the understanding of such diverse biological functions as protein synthesis or signal transduction (1,2). Extended conformational ensembles may be present during membrane insertion and translocation of neurotransmitters targeting G-protein coupled receptors (GPCRs). Whereas the process of membrane insertion and refolding of a peptide has been studied by a variety of biophysical methods (3,4), the structural insight at the level of residue-specific backbone conformations is still limited. Such information may, for example, aid the optimization of the ligand membrane permeability and its stability against proteolytic degradation and is hence, beyond its biological significance, also of considerable pharmacological relevance (5).

Many unbound ligands exhibit an equilibrium mixture of several conformers, thus prohibiting a structural analysis by crystallographic methods. Solution-state NMR methods have been utilized to study peptide structure and hormone receptor interactions on the molecular level (6). Because of the high molecular tumbling rate, such studies have been restricted to approaches that a), examine ligands that interact in low affinity with their GPCR (7), or b), characterize a large number of compounds with a wide variety of biological activities (structure-activity studies) in an aqueous or micellar solution (see, for example, Pellegrini and Mierke (6) and Wüthrich et al. (8)).

Solid-state NMR (ssNMR) provides a spectroscopic means to extend such structural investigations to the case of solid-phase or slowly tumbling systems and was successfully used to analyze conformational distributions of peptides in frozen solutions (9,10) or in large biopolymers (11,12). Although the methods employed in these studies are highly sensitive to the local structure of pairwise isotope labeled peptides, their application to multiply or uniformly labeled systems is not straightforward. High resolution conditions can be established by fast magic angle spinning (MAS (13)), for which a variety of ssNMR schemes probing structural aspects in locally ordered systems have been developed (see Luca et al. (14) for a recent review).

We have recently shown how ssNMR data can be used to probe the structure of the GPCR ligand neurotensin (NT), a 13-amino acid peptide that is involved in a variety of neuromodulatory functions in the central and peripheral nervous system, when bound to its GPCR NTS-1 (15). Not only the full-length peptide, but also the C-terminal part of NT, NT(8–13), has been found to interact with NTS-1 with high affinity. These ssNMR studies speak in favor of an extended, rather well-defined β-strand conformation of receptor-bound NT(8–13).

For an efficient, structure-based pharmacological design, additional information about the conformational ensemble of the free ligand in solution is highly desirable, even if the peptide ligand lacks a well-defined secondary structure and tertiary contacts. A crucial question here is whether the conformational ensemble adopted by the GPCR agonist or antagonist in the lipid phase largely overlaps with the receptor-bound form. Such a conformational preorganization has been suggested as a general ligand-GPCR binding mode (6,16). Previous solution-state NMR studies of NT in aqueous, methanol, and detergent (sodium dodecyl sulfate) solutions (17) indicated an inherent conformational flexibility with no discernible elements of secondary structure in water and methanol and provided no information on the lipid phase. Complementing existing biophysical approaches (18), we show here that ssNMR, optionally combined with submicro-

---

second molecular dynamics (MD) simulations, can be used to study the conformational ensemble adopted by the intrinsically unstructured free NT(8–13) in different environments below the freezing point at the level of individual residues. For this purpose, we make use of the inherent sensitivity of the isotropic chemical shift detected under MAS to molecular structure. In general, the chemical shift not only depends on residue type (19,20) and backbone conformation (20–23), but is also influenced by the nature and structural topology of the neighboring side chains and residues (24,25). Hence, we have developed a strategy that adequately samples the allowed conformational space for a given polypeptide, predicts the backbone chemical shifts C_α and C_β using standard routines, and finally applies a selection criterion based on results of a two-dimensional (2D) ssNMR experiment. For each residue, a particular backbone conformation gives rise to one distinct crosspeak position. Conformational heterogeneity hence translates into 2D crosspeak patterns that provide a spectroscopic snapshot of all backbone conformations present in the polypeptide of interest.

In principle, the signal intensity measured for a given set of NMR frequencies not only encodes information about the backbone structure, but also reports on the probability to find a particular torsion angle value. As demonstrated before, extraction of such angular distribution functions from ssNMR data alone represents, however, an ''ill-posed'' problem and must be aided by further assumptions about the general character of the distribution function (11) or by other techniques such as MD simulations (10). Such an analysis was not attempted here. Instead, we show that the simultaneous spectroscopic analysis of ssNMR data of two or three sequential peptide residues can be used to narrow down the range of dihedral angle values in a disordered solid. The principal use of such a selection criterion is first demonstrated in ubiquitin where structural information is available. Subsequently, this concept is used to investigate the details of NT ligand recognition and, in particular, how the structural ensemble changes from an aqueous solution via detergents into the receptor-bound form. In the case of NT in H_2O at $-50°C$, the ssNMR predictions are compared to independent, restraint-free MD simulations.

METHODS

Sample preparation and ssNMR experiments

The preparation of U-[^{13}C,^{15}N] labeled NT(8–13) as well as the ssNMR experiments and results on detergent-solubilized and receptor-bound NT6 is described in detail in Luca et al. (15). Additional data were recorded on a sample of 4 mg peptide dissolved in water. Similar to other ssNMR applications in aqueous (9,10) or lipid (26,27) environments, this sample was rapidly frozen to $-50°C$ to minimize ice formation during cooling. We note that any cooling rate realizable in a biophysical experiment may be too slow to preserve the conformation of a small molecule. A (DQ (double-quantum)/ZQ(zero-quantum)) (^{13}C,^{13}C) NMR spectrum (28) was recorded on a wide-bore 600 MHz (^{1}H resonance frequency, Bruker, Karlsruhe,

Germany) spectrometer using a double (^{1}H,^{13}C) resonance MAS probe head (Fig. 1). For initial excitation, proton-to-carbon cross-polarization with a contact time of 500 μs was used. Homonuclear mixing in the (DQ/ZQ) (^{13}C,^{13}C) experiment was achieved by proton-driven spin-diffusion with a mixing time of 20 ms.

ssNMR data analysis

Our goal is to retrieve conformational parameters of disordered peptides or proteins using experimental ssNMR data. The general protocol, which we denote for brevity as MC-SAS (Monte Carlo-based structural analysis of ssNMR data) can be applied to any given peptide segment of at least five amino acid residues and consists of three parts: 1), The entire accessible conformational space of the peptide is uniformly sampled by generating a large number of random structures. An algorithm not biased by energy minimization routines is employed. 2), A software routine subsequently predicts chemical shifts of interest for all generated structures. 3), And 2D ssNMR experiments are performed on the given peptide/protein sample. Peptide conformations for which predicted chemical shifts are in agreement with the experiment are selected. From this subensemble of structures, restrictions for various degrees of freedom can be extracted. The individual steps are described in more detail in the following:

1. To create a library of random conformations for a given peptide, we first generate random backbone conformations (random ψ and ϕ torsion angles for all amino acid residues). These are subsequently used as constraints (with $\pm10°$ tolerance) within the computer program CNS (29) to derive three-dimensional (3D) structures. Structures with unphysical geometries were discarded. The resulting libraries encompass several hundred thousand structures and adequately sample the entire (ψ,ϕ) space.

2. Isotropic chemical shifts are predicted for each given 3D structure by the SHIFTX software routine (25) that uses a combination of DFT calculations and empirical NMR data to establish a functional dependence between structure and NMR chemical shifts. The validity of this approach was confirmed by comparing ^{13}C chemical shift predictions for several globular proteins to experimental ssNMR resonance assignments (see Supplementary Material, Table SI1, and Fig. SI1). In line with test applications in the solution state, these studies reveal that the accuracy of the predicted ^{13}C chemical shifts (with root mean-square deviation values of 1.2 ppm for C_α and 1.4 ppm for C_β) is comparable to the natural line width (i.e., ±0.7 ppm) observed in the solid state. In addition, we have shown earlier that solution-state NMR shifts are a viable reference for the analysis of conformation-dependent chemical shifts in the solid state (23).

3. In the experimental 2D spectra a threshold above the noise level is chosen (see Fig. 1 B). Based on amino acid specificity and side-chain correlations, chemical shift assignments were made for each resonance, as depicted in Fig. 1 A for the case of NT(8–13) in frozen solution. Crosspeaks may not be completely resolved (see, for example, $8R_\alpha/9R_\alpha$ and $12I_\alpha/11Y_\alpha$ in Fig. 1) and, therefore, upper and lower limits must be selected for each C_α and C_β chemical shift as indicated in Fig. 1 B. For each amino acid residue, structures are selected that agree with the ssNMR data for the considered and at least one neighboring residue (accuracy ±0.75 ppm), i.e., where the calculated C_α/C_β crosspeaks for at least two neighboring residues must lie inside the contour level at 2.5 times the noise level of the spectrum and within the rectangle defined by the chemical shift limits, as depicted for 11Y in Fig. 1 C. Finally, a Ramachandran plot is generated for each residue, reflecting the number of selected structures within $\pm5°$ of each ϕ,ψ-pair.

A more detailed analysis could take into account exact 2D crosspeak amplitudes. This assumption would require a magnetization transfer rate between C_α and C_β independent of the chemical shifts under the given experimental conditions. Furthermore, even if this information were used, a direct determination of conformational distributions would require further
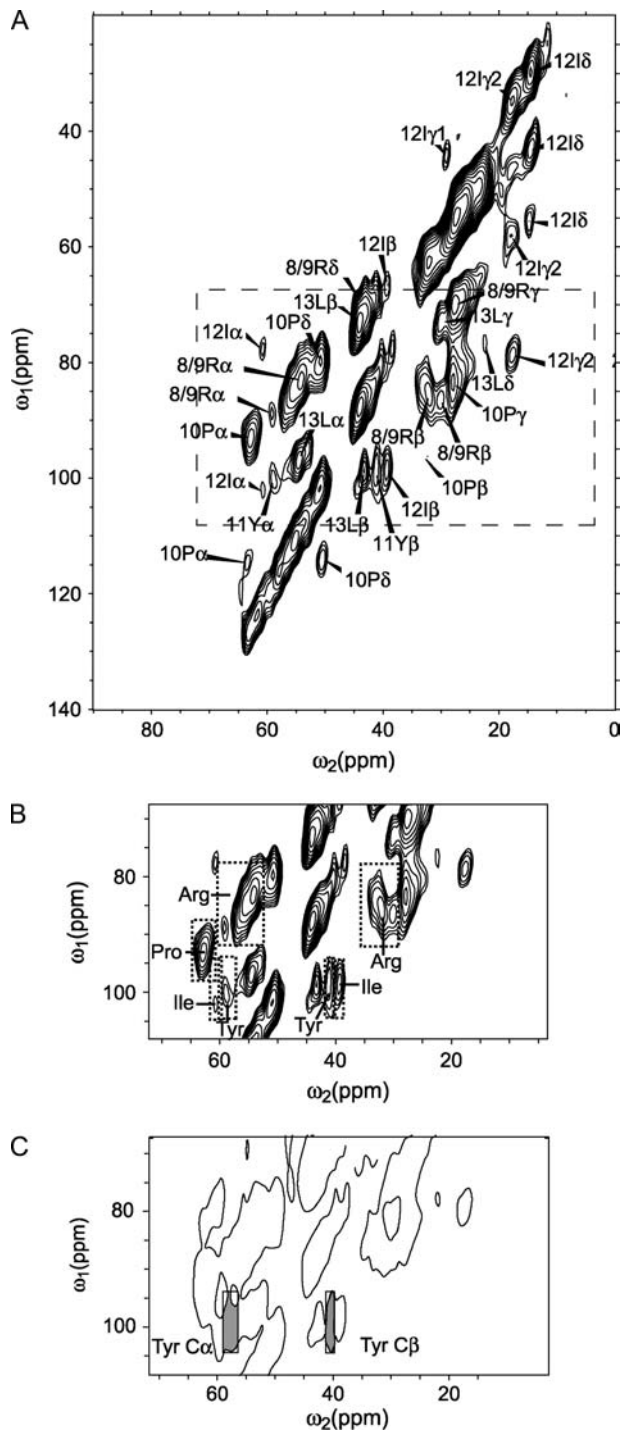
FIGURE 1   DQ/ZQ-spectrum $^{13}C/^{13}C$ (28) of frozen NT(8–13) in flash-frozen aqueous solution. The 2D spectrum was obtained using TPPM decoupling (54) and an MAS rate of 9 kHz on a 600 MHz wide-bore (Bruker Biospin, Karlsruhe, Germany) NMR instrument. Homonuclear mixing was achieved by 20 ms proton-driven spin diffusion. A total of 128 t_1 experiments with 768 scans each were recorded, amounting to a total indirect evolution time of 6.5 ms. (A) Double quantum region of the spectrum encompassing aliphatic ^{13}C resonances with assignments of all resolved crosspeaks. (B) Chemical shift regions for the different amino acids chosen for the selection of the structures. (C) Threshold at 2.5 times the noise level for the selection of structures (C_α/C_β crosspeak region as marked by

assumptions about the character of the distribution function or would be prohibited by spectral resolution. Hence, the color coding given in the Ramachandran plots discussed in the following reflects the number of structural hits obtained from our MC-SAS analysis and does not reveal a direct relation to the distribution function. It is influenced by topological factors including side-chain orientation or backbone conformation of neighboring residues.

From human ubiquitin, the peptide segments (Gly[10]-Glu[16]), (Thr[14]-Glu[24]), and (Lys[27]-Lys[33]), corresponding to β-sheet, loop, and, respectively, α-helical regions, were tested. The hexapeptide (Arg-Arg-Pro-Tyr-Ile-Leu), equivalent to NT(8–13), was investigated immobilized in different chemical environments.

MD simulations

MD simulations were started from a modeled extended conformation of the NT6 peptide. To mimic the experimental conditions, the termini were modeled uncharged by capping the N-terminus with an acetyl group and protonating the C-terminus, respectively. Two simulations were carried out in the GROMOS96 united atom (30) and OPLS all atom force fields (31), respectively. For the OPLS simulation, the peptide was solvated in 2246 TIP4P (32) water molecules. For the GROMOS96 simulation, 2261 SPC (33) water molecules were added as solvent. To both simulation systems, two chloride ions were added to compensate for the net positive charge of the peptide. The total system size comprised 9115 and 6867 atoms for the OPLS and GROMOS96 simulations, respectively. Both MD simulations were carried out using the GROMACS simulation suite (34). Lincs and Settle (35,36) were applied to constrain covalent bond lengths, allowing an integration step of 2 fs. Electrostatic interactions were calculated using the particle mesh ewald method (37). The temperature was kept constant at 300 K by separately coupling ($\tau = 0.1$ ps) the peptide and solvent to an external temperature bath (38). The pressure was kept constant at 1 bar by weak isotropic coupling ($\tau = 1.0$ ps) to a pressure bath. Both simulations were run for 100 ns. For molecular visualization, the pymol program (39) was used.

We consider the generated ensemble sufficiently converged because the observed conformations were visited several times during the simulation, thus indicating reversibility. Furthermore, peptides of similar size have been found previously to exhibit reversible folding dynamics at room temperature at a 100 ns timescale (40). As sufficient sampling would not be expected within the simulation time for the temperature applied in the NMR experiment, a higher temperature (300 K) was chosen for the simulation. As a check, an additional simulation at 280 K was carried out, for which the populations did not change significantly.

RESULTS AND DISCUSSION

The MC-SAS routine

The interpretation of the ssNMR data relies on procedures that directly translate chemical shifts (e.g., of C_α and C_β nuclei) into conformational parameters (here the backbone angles ϕ and ψ). In general, C_α and C_β chemical shifts of an amino acid residue are influenced not only by its backbone and side-chain conformation, but also by the type and structural topology of the neighboring residues. Given the complexity of this functional dependence even for small

---

the rectangle in A): only structures are selected by the MC-SAS approach, for which both C_α/C_β crosspeaks lie inside the contour line and fulfill the chemical shift criterion of B for C_α and C_β shifts, as indicated by the shaded areas for Tyr. The exact chemical shift constraints are given in Table 12 of the supplementary material.

peptides, we employ a Monte Carlo-based structural analysis of protein segments encompassing 6–11 residues. We note that Monte Carlo routines have previously been employed to create solution-state NMR observable parameters, in particular nuclear Overhauser effect intensities, in denatured states of proteins (41).

Our MC-SAS approach was tested by employing three different regions of secondary structure of the globular protein ubiquitin, for which structural information is available (Protein Data Bank entry 1UBQ, 1D3Z). Conformational disorder was simulated assuming chemical shift intervals (±1.5 ppm) that exceed the natural line width of a well-ordered ubiquitin sample in the solid state. Correspondingly, the MC-SAS approach selects allowed backbone angle ranges for all considered residues (Fig. 2). In all cases, backbone angles obtained from the crystal structure (indicated by *bold circles*) are found close to or within regions of high statistical density. Furthermore, there are no qualitative differences between regions of well-defined secondary structure (Ile[13], Ile[30]) and the considered loop region (Glu[16]-Thr[22]) of the protein. These results confirm that the MC-SAS method provides a viable selection criterion to narrow down the backbone torsion angle space of a disordered polypeptide solely based on ssNMR data. Because the chemical shift does not unequivocally define the backbone torsion angle, this method can provide only an upper limit of the conformational space.

Comparison of MC-SAS analysis and MD results on water-solubilized NT(8–13)

An aqueous solution of U-[^{13}C,^{15}N] labeled NT(8–13) was rapidly frozen to −50°C. In agreement with Tycko et al. (42), we experimentally found that the cooling rate does not have a substantial influence on the solid-state 2D NMR spectra. At −50°C, the solution is well below the glass transition, and peptide motions or chemical exchange are assumed to be negligible. The resulting 2D (DQ/ZQ) (^{13}C,^{13}C) correlation spectrum (28) (Fig. 1) was analyzed using the MC-SAS approach and led to the backbone conformational space indicated in Fig. 3 *A*. Similar to the discussion in Luca et al. (15), homonuclear (^{13}C,^{13}C) spectroscopy does not allow for a discrimination of Arg[8] and Arg[9] of NT, hence Fig. 3 contains a superposition of both Arg residues. In general, the MC-SAS method predicts disordered backbone conformations for all considered residue types, with notable exceptions for Pro[10], Tyr[11], and Ile[12] that do not adopt typical left-handed or right-handed α-helical structures, respectively.

Subsequently, we performed a series of MD simulations using the OPLS (Fig. 3 *B*) or the GROMOS96 (Fig. 3 *C*) force field. Interestingly, deviations between both force fields are predominantly observed in the right-handed and left-handed α-helical regions of the Ramachandran histogram. From visual inspection, the agreement between the MC-SAS data and the MD simulations using the OPLS force
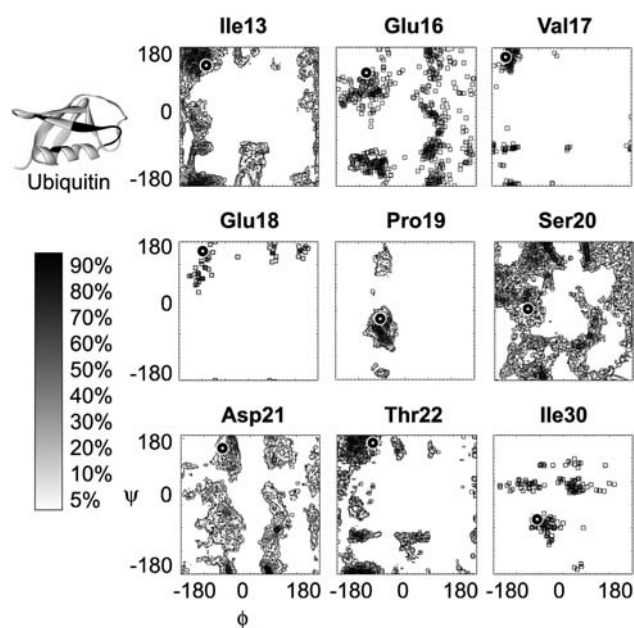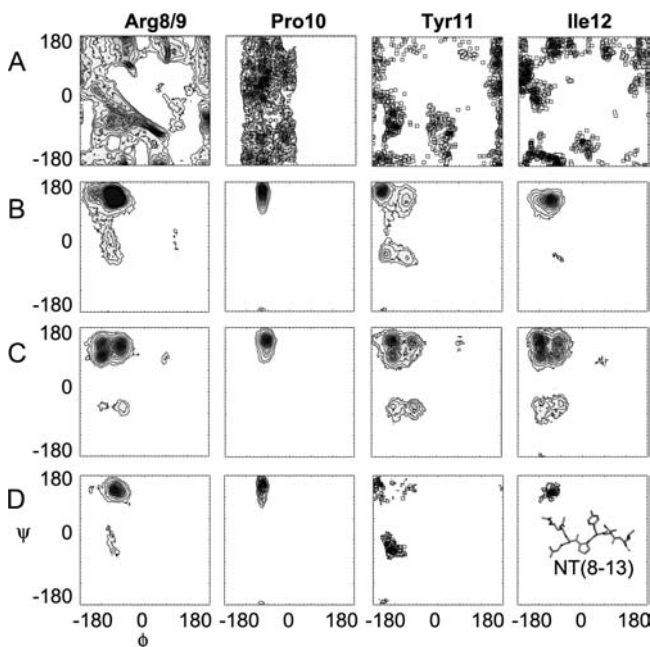
FIGURE 2 Comparison of MC-SAS backbone torsion angle prediction (*shaded*) to structural results (*circle*, Protein Data Bank entry 1UBQ) for selected protein residues (denoted in *black*) of ubiquitin. Contour levels are shown for 5–90% of the maximum number of structural hits. Considered is the loop region (Glu[16]-Thr[22]) and, for reference, two residues (Ile[13] and Ile[30]) found in β-sheet and α-helical segments of the protein, respectively.

FIGURE 3 (*A*) MC-SAS analysis of NT(8–13) in a flash-frozen water solution. Contour levels are shown for 5–90% of the maximum number of structural hits (see Fig. 1 for color scale). (*B* and *C*) Ramachandran plots obtained from MD simulations using the OPLS (31) (*B*) or the GROMOS96 (55) (*C*) force field. (*D*) NMR-consistent conformations weighted with the probability function obtained from the MD/OPLS simulation.

field seems better than for the GROMOS96 force field. This is quantified by the correlation functions between MC-SAS and the corresponding MD Ramachandran matrices, which are increased from g96 to OPLS by 8% (Arg[8/9]), 22% (Pro[10]), 30% (Tyr[11]), and 75% (Ile[12]). In addition, chemical shift correlations derived for OPLS-based peptide structures agree better with experimental data, albeit with a smaller overall difference between both force fields (see Supplementary Material, Table SI3, and Fig. SI2). Hence, in the following, we shall concentrate on the MD/OPLS results. The conformational space consistent with the chemical shifts is restricted further, taking the MD results into account. In Fig. 3 D the NMR-allowed torsion angle space of Fig. 3 A is weighted with the probability function from the MD simulations in Fig. 3 B. In general, all residues considered display a propensity for β-strand conformations (43). Notably, significant populations of α-helical regions are observed for Tyr[11] and at least for one of the Arg residues.

Fig. 4 shows a conformational comparison of the structures sampled by the MC-SAS procedure and the OPLS-based MD simulation. Each of the spheres shown represents an individual conformation sampled by the different procedures, projected onto the three principal modes of collective backbone fluctuations, as determined by a principal component analysis of the full ensemble (44,45). As can be seen, the most extended ensemble is sampled by the MC-SAS procedure (*magenta spheres*), which also includes configurations that are not visited during the MD simulation (*blue spheres*). In red and orange, those MD configurations are depicted that match the measured chemical shift ranges exactly (*red*) and within a tolerance range of ± 0.5ppm (*orange*). The second largest conformational cluster (*right* in
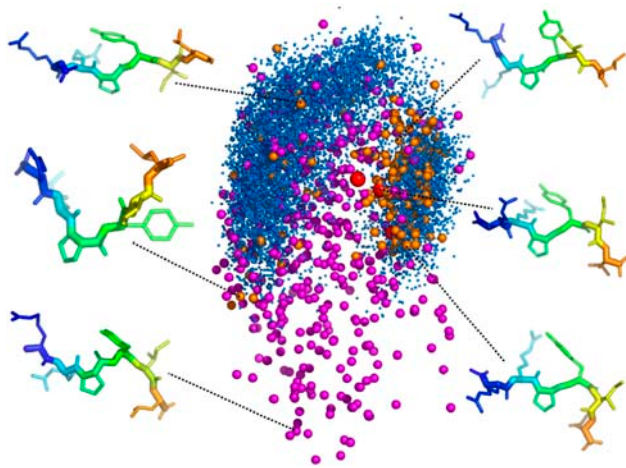

FIGURE 4 Sampled conformational space and selected snapshots from the MC-SAS and MD/OPLS structural ensembles. The spheres represent individual configurations projected onto the three principal modes of collective fluctuation as obtained from a principal component analysis. Shown are MC-SAS structures (*magenta*), MD/OPLS structures (*blue*), and a selection of MD/OPLS structures that are strictly (*red*) or less strictly (*orange*) consistent with the NMR data.

Fig. 4) contains structures that are in close agreement with the experimentally measured chemical shifts. This region corresponds largely to an extended conformation with a bend in the backbone near Tyr[11]. Interestingly, the conformation most frequently visited during the simulation, a fully extended conformation (*left* in Fig. 4), contains only a few structures that are in agreement with the NMR data. The apparent discrepancy that this most frequently sampled structure is not the one that matches the ssNMR data best may be partially explained by the fact that the ssNMR experiments were conducted at $-50°$C, whereas the simulations were necessarily conducted at room temperature. The conformations that are allowed by the MC-SAS procedure but are not sampled during the simulation (Fig. 4, *bottom*) correspond to structures with Pro[10] in a *cis* configuration, which are not excluded by the MC-SAS approach. The close proximity of the backbone carbonyl oxygen atoms of Arg[9] and Pro[10] in this configuration makes these structures energetically unfavorable. Moreover, in line with these energetic considerations, C_γ chemical shifts values are found that speak against Pro[10] *cis* conformations of NT(8–13) in H_2O (46).

Changes of the backbone of conformation NT(8–13) upon binding

Finally, we applied the MC-SAS approach to compare the backbone dihedral angle space sampled by NT(8–13) in water (Fig. 5 A) to results obtained in model lipids (Fig. 5 B) and to the MC-SAS-allowed conformations in the receptor-bound form (Fig. 5 C). Consistent with the TALOS (24) analysis used in Luca et al. (15) (which analyzes NMR chemical shift assignments of three consecutive peptide residues by using a statistical homology search), the receptor-bound conformation of NT(8–13) is largely found
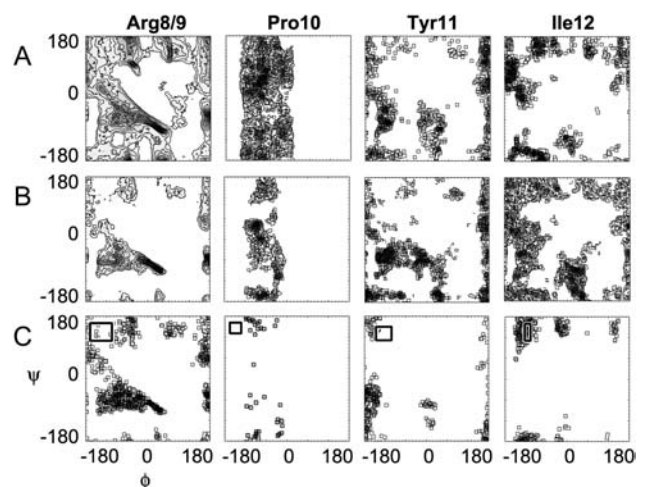

FIGURE 5 NMR-allowed conformations of NT(8–13) in aqueous solution (A), in detergents (B), and in the receptor-bound form (C). The torsion angle range predicted by TALOS for the receptor-bound form is indicated by black/white squares.

in the β-sheet region of the Ramachandran plot. On the other hand, the conformational space allowed for NT(8–13) in model lipids is significantly larger than in the receptor-bound form and encompasses large regions that are excluded in the receptor-bound form. Furthermore, we observe a remarkable correlation between the distribution functions obtained in the presence of detergents to the situation in H_2O: Whereas the allowed Ramachandran region in Fig. 5 *B* is considerably larger for the hydrophobic residues Tyr[11] and Ile[12], the available conformational space for Arg and Pro is smaller in model lipids (4). In general, left-handed α-helical structures are not observed for Tyr[11] or Ile[12]. On the other hand, right-handed α-helical regions remain accessible for all considered residue types. As can be seen from Fig. 5, a detailed analysis of Arg[8/9] is not possible, most likely due to inherent flexibility of Arg[8] that obscures a further analysis of Arg[9]. Here, additional $^{15}N/^{13}C$ correlation experiments could help to reduce the ambiguity of the retrieved results.

CONCLUSIONS

Using ssNMR, we have investigated the conformational space adopted by the intrinsically unstructured ligand peptide NT(8–13) in a frozen aqueous solution, in a model lipid environment, and in its receptor-bound form. Our analysis makes use of the well-established dependency between (C_α,C_β) chemical shifts and protein secondary structure. The MC-SAS approach can be used if spectral resolution is sufficient to obtain (C_α,C_β) chemical shift assignments under MAS conditions and does not require additional biophysical data to confine the conformational space of backbone torsion angles in disordered peptides. On the other hand, this method must be complemented by additional structural parameters if a de novo structure determination of a well-ordered peptide is attempted. For an aqueous solution of NT(8–13), we restricted the conformational space further by including ensembles from MD simulations to eliminate NMR-allowed, but physically unlikely structures. Although the NT peptide is largely unstructured in aqueous solution, our NMR and MD data show that it only adopts a small subset of all possible backbone conformations, as it has also been observed for β peptides (40). In addition, comparison between structural ensembles derived from experimental data and simulations provided a rigorous test for MD force fields. Here, for NT in H_2O, the experimental results are in better agreement with MD simulations using the OPLS force field than for the GROMOS96 force field.

In the model lipid environment, in which the receptor has been shown to be functional, the degree of conformational flexibility of NT(8–13) changes in a residue-specific manner. Whereas the degree of disorder increases for the lipophilic residues, the distribution profile of allowed Ramachandran entries for Arg and Pro narrows compared to the results obtained in H_2O. Notably, these observations agree with whole-residue hydrophobicity scales reported for a transfer from water to a lipid interface (4). The conformational space of the receptor-bound peptide shows only little overlap with that adopted in the lipid environment. These observations speak against a ligand conformational preorganization of NT such as recently proposed for peptide hormones interacting with receptors of the type B GPCR family (7) and is hypothesized as a general ligand-GPCR binding mode (6,16).

Our ssNMR approach provides an upper boundary for the conformational space adopted by disordered peptides and provides, possibly in conjunction with MD simulations, insight into the details of protein folding. The conformational analysis presented here relies on the relationship between protein structure and the chemical shift detected for a given peptide during the ssNMR experiment. Similar to the TALOS approach, the allowed conformational space is refined by considering simultaneously results of two or three sequential residues. Anisotropic tensor correlation methods (10,11,47) could offer higher structural resolution, but they would require the analysis of several selectively labeled protein variants. In principle, redundancies in the chemical shift hypersurface could be further minimized by an extended MC-SAS approach that incorporates the measurement of molecular torsion angles (48–50) or internuclear distances (51–53) under high-resolution ssNMR conditions.

SUPPLEMENTARY MATERIAL

An online supplement to this article can be found by visiting BJ Online at http://www.biophysj.org.

REFERENCES

1. Radford, S. E., and C. M. Dobson. 1999. From computer simulations to human disease: emerging themes in protein folding. *Cell.* 97:291–298.

2. Wright, P. E., and H. J. Dyson. 1999. Intrinsically unstructured proteins: re-assessing the protein structure-function paradigm. *J. Mol. Biol.* 293:321–331.

3. Ladokhin, A. S., and S. H. White. 2004. Interfacial folding and membrane insertion of a designed helical peptide. *Biochemistry.* 43:5782–5791.

4. White, S. H., and W. C. Wimley. 1999. Membrane protein folding and stability: physical principles. *Annu. Rev. Biophys. Biomol. Struct.* 28:319–365.

5. Hruby, V. J. 2002. Designing peptide receptor agonists and antagonists. *Nat. Rev. Drug Discov.* 1:847–858.

6. Pellegrini, M., and D. F. Mierke. 1999. Structural characterization of peptide hormone/receptor interactions by NMR spectroscopy. *Biopolymers.* 51:208–220.

7. Inooka, H., T. Ohtaki, O. Kitahara, T. Ikegami, S. Endo, C. Kitada, K. Ogi, H. Onda, M. Fujino, and M. Shirakawa. 2001. Conformation of a peptide ligand bound to its G-protein coupled receptor. *Nat. Struct. Biol.* 8:161–165.

8. Wüthrich, K., C. Bosch, and L. R. Brown. 1980. Conformational studies of lipid-bound polypeptides by elucidation of proton-proton cross-relaxation networks. *Biochem. Biophys. Res. Commun.* 95:1504–1509.

9. Smith, L. J., F. P. Boulineau, D. Raftery, and A. Wei. 2003. Frozen-solution conformational analysis by REDOR spectroscopy. *J. Am. Chem. Soc.* 125:14958–14959.

10. Long, H. W., and R. Tycko. 1998. Biopolymer conformational distributions from solid-state NMR: alpha-helix and 3(10)-helix contents of a helical peptide. *J. Am. Chem. Soc.* 120:7039–7048.

11. van Beek, J. D., L. Beaulieu, H. Schafer, M. Demura, T. Asakura, and B. H. Meier. 2000. Solid-state NMR determination of the secondary structure of Samia cynthia ricini silk. *Nature.* 405:1077–1079.

12. van Beek, J. D., S. Hess, F. Vollrath, and B. H. Meier. 2002. The molecular structure of spider dragline silk: folding and orientation of the protein backbone. *Proc. Natl. Acad. Sci. USA.* 99:10266–10271.

13. Andrew, E. R., A. Bradbury, and R. G. Eades. 1958. Nuclear magnetic resonance spectra from a crystal rotated at high speed. *Nature.* 182:1659.

14. Luca, S., H. Heise, and M. Baldus. 2003. High-resolution solid-state NMR applied to polypeptides and membrane proteins. *Acc. Chem. Res.* 36:858–865.

15. Luca, S., J. F. White, A. K. Sohal, D. V. Filippov, J. H. van Boom, R. Grisshammer, and M. Baldus. 2003. The conformation of neurotensin bound to its G protein-coupled receptor. *Proc. Natl. Acad. Sci. USA.* 100:10706–10711.

16. Schwyzer, R. 1995. 100 years lock-and-key concept: are peptide keys shaped and guided to their receptors by the target-cell membrane? *Biopolymers.* 37:5–16.

17. Xu, G. Y., and C. M. Deber. 1991. Conformations of neurotensin in solution and in membrane environments studied by 2-D NMR-spectroscopy. *Int. J. Pept. Protein Res.* 37:528–535.

18. Fersht, A. R., and V. Daggett. 2002. Protein folding and unfolding at atomic resolution. *Cell.* 108:573–582.

19. Cavanagh, J., W. J. Fairbrother, A. G. Palmer, and N. J. Skelton. 1996. Protein NMR Spectroscopy. Principles and Practice. Academic Press, San Diego, CA.

20. Saito, H. 1986. Conformation-dependent ^{13}C chemical shifts—A new means of conformational characterization as obtained by high-resolution solid-state ^{13}C NMR. *Magn. Reson. Chem.* 24:835–852.

21. Laws, D. D., H. M. L. Bitter, K. Liu, H. L. Ball, K. Kaneko, H. Wille, F. E. Cohen, S. B. Prusiner, A. Pines, and D. E. Wemmer. 2001. Solid-state NMR studies of the secondary structure of a mutant prion protein fragment of 55 residues that induces neurodegeneration. *Proc. Natl. Acad. Sci. USA.* 98:11686–11690.

22. Spera, S., and A. Bax. 1991. Empirical correlation between protein backbone conformation and C_α and C_β ^{13}C nuclear magnetic resonance chemical shifts. *J. Am. Chem. Soc.* 113:5490–5492.

23. Luca, S., D. V. Filippov, J. H. van Boom, H. Oschkinat, H. J. M. de Groot, and M. Baldus. 2001. Secondary chemical shifts in immobilized peptides and proteins: a qualitative basis for structure refinement under magic angle spinning. *J. Biomol. NMR.* 20:325–331.

24. Cornilescu, G., F. Delaglio, and A. Bax. 1999. Protein backbone angle restraints from searching a database for chemical shift and sequence homology. *J. Biomol. NMR.* 13:289–302.

25. Neal, S., A. M. Nip, H. Y. Zhang, and D. S. Wishart. 2003. Rapid and accurate calculation of protein H-1, C-13 and N-15 chemical shifts. *J. Biomol. NMR.* 26:215–240.

26. Cross, T. A., and J. R. Quine. 2000. Protein structure in anisotropic environments: development of orientational constraints. *Concepts Magn. Reson.* 12:55–70.

27. Sizun, C., and B. Bechinger. 2002. Bilayer sample for fast or slow magic angle oriented sample spinning solid-state NMR spectroscopy. *J. Am. Chem. Soc.* 124:1146–1147.

28. Luca, S., and M. Baldus. 2002. Enhanced spectral resolution in immobilized peptides and proteins by combining chemical shift sum and difference spectroscopy. *J. Magn. Reson.* 159:243–249.

29. Brünger, A. T., P. D. Adams, G. M. Clore, W. L. DeLano, P. Gros, R. W. Grosse-Kunstleve, J. S. Jiang, J. Kuszewski, M. Nilges, N. S. Pannu, R. J. Read, L. M. Rice, T. Simonson, and G. L. Warren. 1998. Crystallography & NMR system: a new software suite for macromolecular structure determination. *Acta Crystallogr. Sect. D Biol. Crystallogr.* 54:905–921.

30. Van Gunsteren, W. F., S. R. Billeter, A. A. Eising, P. Huenenberger, A. E. Mark, W. R. P. Scott, and I. G. Tironi. 1996. Biomos. Groningen, Zurich.

31. Jorgensen, W. L., D. S. Maxwell, and J. Tirado-Rives. 1996. Development and testing of the OPLS all-atom force field on conformational energetics and properties of organic liquids. *J. Am. Chem. Soc.* 118:11225–11236.

32. Jorgensen, W. L., J. Chandrasekhar, J. D. Madura, R. W. Impey, and M. L. Klein. 1983. Comparison of simple potential functions for simulating liquid water. *J. Chem. Phys.* 79:926–935.

33. Berendsen, H. J. C., J. P. M. Postma, W. F. van Gunsteren, and J. Hermans. 1981. Intermolecular Forces. D. Reidel Publishing Company, Dordrecht, The Netherlands. 331–342.

34. Lindahl, E., B. Hess, and D. van der Spoel. 2001. GROMACS 3.0: a package for molecular simulation and trajectory analysis. *J. Mol. Model.* 7:306–317.

35. Hess, B., H. Bekker, H. J. C. Berendsen, and J. Fraaije. 1997. LINCS: a linear constraint solver for molecular simulations. *J. Comput. Chem.* 18:1463–1472.

36. Miyamoto, S., and P. A. Kollman. 1992. Settle—an analytical version of the shake and rattle algorithm for rigid water models. *J. Comput. Chem.* 13:952–962.

37. Darden, T., D. York, and L. Pedersen. 1993. Particle mesh ewald—an N.log(N) method for ewald sums in large systems. *J. Chem. Phys.* 98:10089–10092.

38. Berendsen, H. J. C., J. P. M. Postma, W. F. Vangunsteren, A. Dinola, and J. R. Haak. 1984. Molecular-dynamics with coupling to an external bath. *J. Chem. Phys.* 81:3684–3690.

39. DeLano, W. L. 2002. The PyMOL Molecular Graphics System. DeLano Scientific, San Carlos, CA. http://www.pymol.org.

40. Daura, X., B. Jaun, D. Seebach, W. F. van Gunsteren, and A. E. Mark. 1998. Reversible peptide folding in solution by molecular dynamics simulation. *J. Mol. Biol.* 280:925–932.

41. Fiebig, K. M., H. Schwalbe, M. Buck, L. J. Smith, and C. M. Dobson. 1996. Toward a description of the conformations of denatured states of proteins. Comparison of a random coil model with NMR measurements. *J. Phys. Chem.* 100:2661–2666.

42. Havlin, R. H., and R. Tycko. 2005. Probing site-specific conformational distributions in protein folding with solid-state NMR. *Proc. Natl. Acad. Sci. USA.* 102:3284–3289.

43. Street, A. G., and S. L. Mayo. 1999. Intrinsic beta-sheet propensities result from van der Waals interactions between side chains and the local backbone. *Proc. Natl. Acad. Sci. USA.* 96:9074–9076.

44. Amadei, A., A. B. M. Linssen, and H. J. C. Berendsen. 1993. Essential dynamics of proteins. *Proteins Struct. Funct. Genet.* 17:412–425.

45. Garcia, A. E. 1992. Large-amplitude nonlinear motions in proteins. *Phys. Rev. Lett.* 68:2696–2699.

46. Dorman, D. E., and F. A. Bovey. 1973. C-13 magnetic-resonance spectroscopy—spectrum of proline in oligopeptides. *J. Org. Chem.* 38:2379–2383.

47. Tomaselli, M., P. Robyr, B. H. Meier, C. GrobPisano, R. R. Ernst, and U. W. Suter. 1996. Quantification of conformational disorder in glassy polycarbonate by two-dimensional nuclear magnetic resonance spectroscopy. *Mol. Phys.* 89:1663–1694.

48. Feng, X., Y. K. Lee, D. Sandstrom, M. Eden, H. Maisel, A. Sebald, and M. H. Levitt. 1996. Direct determination of a molecular torsional angle by solid-state NMR. *Chem. Phys. Lett.* 257:314–320.

49. Costa, P. R., J. D. Gross, M. Hong, and R. G. Griffin. 1997. Solid-state NMR measurement of ψ in peptides: a NCCN 2Q-heteronuclear local field experiment. *Chem. Phys. Lett.* 280:95–103.

50. Hong, M., J. D. Gross, and R. G. Griffin. 1997. Site-resolved determination of peptide torsion angle phi from the relative orientations of backbone N-H and C-H bonds by solid-state NMR. *J. Phys. Chem. B.* 101:5869–5874.

51. Bower, P. V., N. Oyler, M. A. Mehta, J. R. Long, P. S. Stayton, and G. P. Drobny. 1999. Determination of torsion angles in proteins and peptides using solid state NMR. *J. Am. Chem. Soc.* 121:8373–8375.

52. Lange, A., S. Luca, and M. Baldus. 2002. Structural constraints from proton-mediated rare-spin correlation spectroscopy in rotating solids. *J. Am. Chem. Soc.* 124:9704–9705.

53. Lange, A., K. Seidel, L. Verdier, S. Luca, and M. Baldus. 2003. Analysis of proton-proton transfer dynamics in rotating solids and their use for 3D structure determination. *J. Am. Chem. Soc.* 125:12640–12648.

54. Bennett, A. E., C. M. Rienstra, M. Auger, K. V. Lakshmi, and R. G. Griffin. 1995. Heteronuclear decoupling in rotating solids. *J. Chem. Phys.* 103:6951–6958.

55. Van Gunsteren, W. F., S. R. Billeter, A. A. Eising, P. Huenenberger, A. E. Mark, W. R. P. Scott, and I. G. Tironi. 1996. Biomolecular Simulation: the GROMOS96 Manual and User Guide. Biomos B.v., Zurich, Groningen, The Netherlands.